

Forecasting the evolution of the current unrest of Campi Flegrei by defining anomalies through experts' elicitation

Salvatore Ferrara¹, Jacopo Selva^{*,2}, Laura Sandri³, Warner Marzocchi^{1,2},
Elicitation VI Working Group⁴

⁽¹⁾ Scuola Superiore Meridionale, Napoli, Italy

⁽²⁾ Università degli Studi di Napoli Federico II, Dipartimento di Scienze della Terra, dell'Ambiente e delle Risorse, Napoli, Italy

⁽³⁾ Istituto Nazionale di Geofisica e Vulcanologia, Sezione di Bologna, Bologna, Italy

⁽⁴⁾ The complete list of the participants can be found in the Appendix

Article history: received September 04, 2024; accepted January 20, 2025

Abstract

The Campi Flegrei caldera, Italy, is considered one of the most high-risk volcanic areas on the planet due to its location within the metropolitan area of Naples. Campi Flegrei caldera is currently undergoing unrest. The unrest is linked to an uplift phase that started in 2005, which is accompanied by gas emissions and volcano-tectonic seismicity. Owing to the limited knowledge of the plumbing system and the pre-eruptive processes, tracking the evolution of a volcanic unrest is often based on probabilities obtained by experts' elicitation. In this work, we present the daily variation of the probability that the unrest is driven by a shallow magma movement and the monthly probability of eruption based on the Bayesian Event Tree for Eruption Forecasting (BET_EF) model calibrated for Campi Flegrei by means of the outcomes of the VI experts' elicitation carried out in 2015. The results show that according to the interpretive framework provided by experts, the probability that the mechanism behind the current unrest is shallow magma movements is not negligible, but the monthly probability of eruption remained overall constant during the entire period.

Keywords: Volcanic hazard; Eruption forecasting; Unrest; Probability; Campi Flegrei

1. Introduction

The Campi Flegrei caldera is a volcano located west of Naples, Italy, which has been active for more than 80,000 years (Scarpati et al., 2013; Vineberg et al., 2023; Fernandez et al., 2024; Sparice et al., 2024). The volcano has experienced several eruptions throughout the Holocene, with the last major event, Agnano Monte Spina, about 4,550 years ago (Orsi et al., 2009; Smith et al., 2011; Bevilacqua et al., 2016). Its latest eruptive event (Monte Nuovo) occurred in 1538 AD (Di Vito et al., 1987, 2016) and represents the only historically documented eruption of the

volcano. After the Monte Nuovo eruption the caldera went into a subsidence state that lasted till the 40s of the last century (Parascandola, 1947; Todesco et al., 2014; Ricco et al., 2019; Vitale and Natale, 2023), when the ground started uplifting again (Orsi et al., 1999).

Campi Flegrei is currently undergoing an unrest phase (D’Auria et al., 2011, 2015; Lima et al., 2021) which is characterized by an almost continuous uplift going on since 2005 (Trasatti et al., 2015; De Martino et al., 2021), continuous gas emissions (Chiodini et al., 2021; Isaia et al., 2021) and swarms of volcano-tectonic earthquakes (VTs) (Giudicepietro et al., 2020, 2021; Ricciolino and Lo Bascio, 2021; Tramelli et al., 2021, 2022, 2024), with a marked accelerating behavior of both uplift and seismicity (Chiodini et al., 2016, 2017; Bevilacqua et al., 2024; Bollettini INGV, 2024).

The ambiguity in the interpretation of the patterns of pre-eruptive phenomena, combined with the complexity of volcanic processes, introduces important uncertainties (Rosi et al., 2022; Acocella et al., 2024), especially for volcanoes that, like Campi Flegrei, have never had a monitored unrest episode that culminated into an eruption, even though significant efforts have been made in reconstructing the pre-eruptive dynamics that occurred in the decades preceding the Monte Nuovo eruption (Guidoboni and Ciuccarelli, 2011; Di Vito et al., 2016).

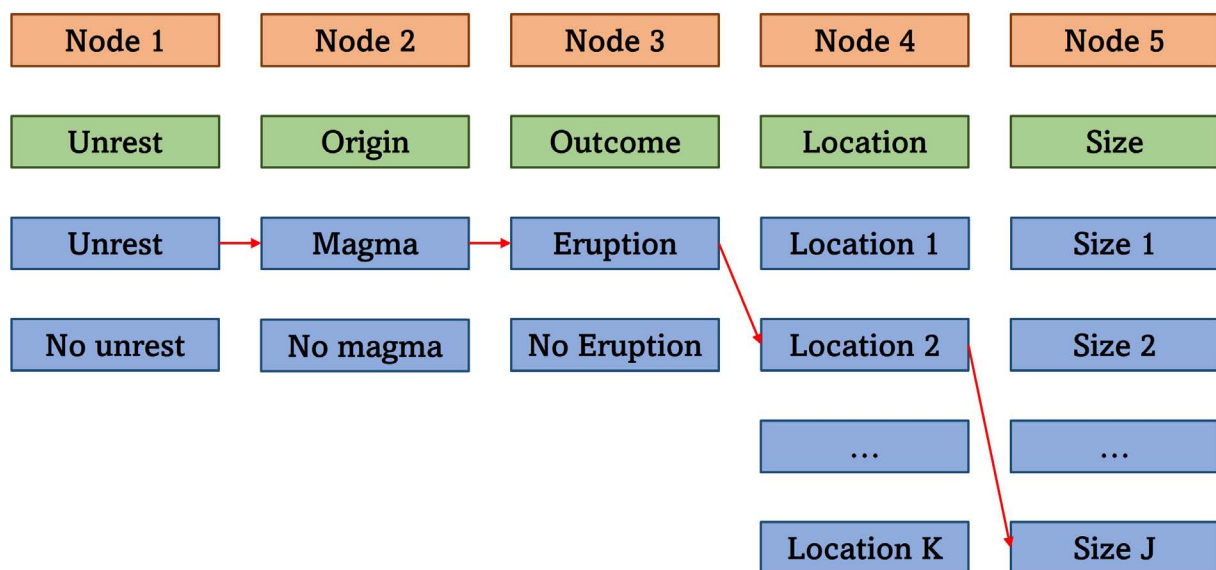


Figure 1. Structure of the Bayesian Event Tree for Eruption Forecasting (BET_EF).

While qualitative assessments can prove effective in specific real-world scenarios, comprehensive risk reduction strategies should rely exclusively on quantitative probabilistic studies (Marzocchi and Woo, 2007, 2009; Marzocchi et al., 2012, 2021; Papale, 2017). Through the introduction of the Bayesian Event Tree (BET) and the Bayesian Event Tree for Eruption Forecasting (BET_EF) (Fig. 1), Marzocchi et al. (2004, 2008) have proposed a method to decompose the calculation of the probability for each specific volcanic event of interest into a chain of conditional probabilities. This is achieved by organizing them into a sequence of nodes within the event tree. The first three nodes of the event tree specifically pertain to eruption forecasting: Node 1 represents “unrest in the next month,” Node 2 signifies “presence of moving shallow magma given unrest,” and Node 3 denotes “eruption in the next month given the presence of magmatic unrest”. The short-term forecast of BET_EF is based on the automatic interpretation of the monitoring observations, based on their comparison with predefined thresholds. The selection of the informative observations at each node and of the corresponding thresholds to define anomalies for Campi Flegrei has been made through a community-based setting based on experts’ elicitation (Selva et al., 2012, 2015). Specifically, here we use the parameters and thresholds that were defined during the last elicitation (the VI elicitation) carried out in 2015.

In this specific application, since the volcano is in a phase of unrest, we focus on nodes 2 and 3 of the event tree. Indeed, our aim is to determine the probability that the mechanism that drives unrest is shallow magma movement, and the probability that this eventual magma movement will lead to an eruption. Remarkably, to our knowledge this is the only tool that has been providing real-time probabilities since the start of this phase of unrest.

2. Methods

Within the event tree, individual probabilities are not represented as single values, but as random variables. This approach allows the consideration of both aleatory and epistemic uncertainties (Marzocchi et al., 2021), which are respectively represented by the mean and the variance of the corresponding probability density function. Aleatory uncertainty is linked to the intrinsic randomness of natural events, while epistemic uncertainty is linked to the lack of knowledge about the event we are dealing with. In our case, aleatory uncertainty represents the uncertainty on the potential outcome of any precursory pattern, while epistemic uncertainty represents the divergence of scientists' opinions linked to the ambiguity in the interpretation of precursor phenomena.

The probability at nodes 2 and 3 of the event tree is described by a beta distribution (Marzocchi et al., 2008). The beta distribution is frequently selected to describe uncertainties in natural hazard forecasting, due to its definition in the $[0,1]$ interval and its property of being the conjugate distribution in the binomial model (Gelman, 1995). The parameters of the beta distribution can be assessed by making use of experts' elicitation (Cooke, 1991; Aspinall, 2006; Selva et al., 2012; Christophersen et al., 2018) and can be updated using data related to past unrest and eruptions (if available).

The expected value (i.e., the mean) of the distribution can be assessed by translating monitoring anomaly observations into probabilities through an entropy-based approach (Marzocchi et al., 2008, 2024). This approach makes use of fuzzy logic (Zadeh, 1965), meaning that each monitoring measurement is assigned a degree of anomaly (z) based on the membership function to the class of anomalous values. Thus, by defining two threshold values, a monitoring observation may be either certainly non-anomalous ($z = 0$), or certainly anomalous ($z = 1$), or it can be characterized by an intermediate and uncertain anomaly state that can be tracked by a given degree of anomaly ($0 < z < 1$). Following the formulation of Marzocchi et al. (2024), a possible definition of a smooth membership has been proposed in Marzocchi et al. (2008):

$$z_i = \begin{cases} 1 & \text{if } a_i \geq a_{max} \\ \frac{1}{2} \left\{ \sin \left[\pi \frac{(a_i - a_{min})}{(a_{max} - a_{min})} - \frac{\pi}{2} \right] + 1 \right\} & \text{if } a_{min} < a_i < a_{max} \\ 0 & \text{if } a_i \leq a_{min} \end{cases} \quad (1)$$

where a_{min} and a_{max} represent the minimum and maximum thresholds for the monitoring variable, respectively, that define when the parameter is considered certainly anomalous or not anomalous (Fig. 2). If $a_{min} = a_{max}$, the uncertainty on the definition of the anomaly becomes 0, and z can only have 0 or 1 values. The definition in Eq. (1) is valid for parameters that exhibit anomalous values for large values (for values larger than the thresholds), but an analogous definition is possible for the parameters that are anomalous for small values (for values smaller than the thresholds).

At this stage, all monitoring information related to a specific node (magmatic unrest or eruption) is condensed within a single parameter known as the "anomaly score" (Z):

$$Z = \sum_{i=1}^N z_i \omega_i \quad (2)$$

where ω_i represents the weight of the i -th anomaly at the BET node under consideration. Subsequently, the information contained within the anomaly score can be used to track the evolution of the expected value of the probability of magmatic unrest or eruption through the following relationship:

$$E[\Phi] = 1 - ae^{-Z} \quad (3)$$

where Φ is the random variable, which is itself a probability, and ' a ' is a parameter used to set the minimum value of the conditional probability of magmatic unrest or eruption when the volcano monitoring system does not

indicate any anomaly ($Z = 0$). The latter parameter has a double purpose: firstly, it acts as a “confidence level” in the monitoring system, as higher values of ‘ a ’ mean lower values of the probability when no anomalies are detected: the better the monitoring system, the larger ‘ a ’. Secondly, if our aim is to forecast the onset of an eruption in a given time window, it considers the possibility that the situation evolves within this time frame: the longer the time window, the lower ‘ a ’.

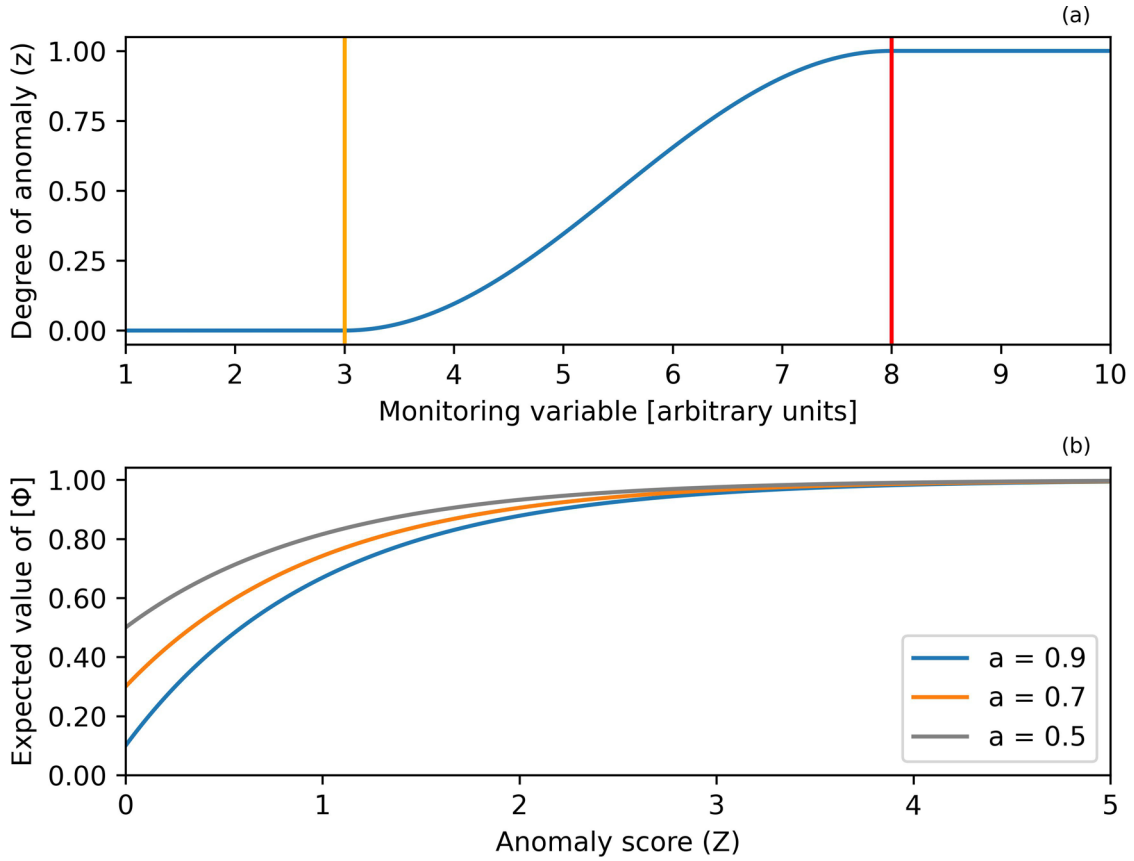


Figure 2. Procedure for obtaining probabilities from monitoring anomaly observations. (a) Transformation of a monitoring measurement into its corresponding degree of anomaly (Eq. 1). If the monitoring measurement falls below the lower threshold (orange line), it will be considered non-anomalous. If it falls between the two thresholds, it will be considered partially anomalous. If it falls above the upper threshold (red line), it will be considered totally anomalous. Subsequently, the anomaly score is computed (Eq. 2). (b) Relationship between the anomaly score (Z) and the expected value of the distribution of magmatic unrest or eruption (Eq. 3), using three different values of ‘ a ’. The plot highlights that the most significant differences are obtained for $Z = 0$. As the anomaly score increases, the differences diminish until approaching 0.

The uncertainty on ϕ can be modelled with a beta distribution whose parameters may be set as:

$$\alpha = E[\Phi] \left(\frac{E[\Phi](1 - E[\Phi])}{\sigma^2} - 1 \right) \tag{4a}$$

$$\beta = (1 - E[\Phi]) \left(\frac{E[\Phi](1 - E[\Phi])}{\sigma^2} - 1 \right) \tag{4b}$$

where σ^2 represents the variance of the distribution of the random variable ϕ . In our case, we do not have multiple estimates of the parameter value but simply the mean value obtained through Eq. (3). A convenient way to express

the variance of the distribution is through the equivalent number of data (Λ) (see Appendix A, Marzocchi et al., 2008). The maximum achievable variance is established when $\Lambda = 1$, indicating that the information matches that of a single datum, while a higher value of Λ corresponds to a lower variance of the distribution and, consequently, a reduced epistemic uncertainty. Through $E[\Phi]$ and Λ we can easily obtain the parameters of the distribution by inverting the following equations:

$$E[\Phi] = \frac{\alpha}{\alpha + \beta} \quad (5)$$

$$\Lambda = \alpha + \beta - 1 \quad (6)$$

In this way, we have at our disposal a probability distribution that accurately describes uncertainties.

The definition of operational unrest is ambiguous, being subjective as any definition of background. A possible degree of unrest may be based on monitoring observations (Marzocchi et al., 2008), that is:

$$\eta = 1 - \prod_{i=1}^{N^{(1)}} (1 - z_i^{(1)}) \quad (7)$$

where the $z_i^{(1)}$ s are the degrees of anomaly of the parameters considered at Node 1 of BET_EF. Eq. (7) tells us that if at least one parameter at Node 1 is found to be totally anomalous, then the volcano will be considered to be in a phase of operational unrest.

3. Calibrating BET_EF through experts' elicitation

BET_EF was calibrated for Campi Flegrei through several elicitation sessions, with six sessions organized between 2005 and 2015 (Selva et al., 2012, 2015). The goal of the elicitation was to define parameters for managing monitoring measures at the first 4 nodes of the model, as in the current state of the art, reliable precursors of the eruption's size do not exist. It is important to stress that all these experts' elicitation experiments were conducted in advance of the present crisis that is the focus of this paper.

In short, all experiments included three different phases:

- A preparatory phase.
- The actual elicitation experiment.
- A post-processing phase.

The preparatory phase consisted of a series of presentations regarding the possible conceptual models of the Campi Flegrei caldera and its behavior, the monitoring system and its sensitivity, the objectives of the elicitation, the methods behind the experiment, the connection between the elicitation results and BET_EF, the results of the previous elicitation sessions, and the list of parameters selectable by the experts. Each of these presentations has been followed by a general discussion.

During the actual experiment, each expert could vote for up to a maximum of five colleagues whom he or she believed to be the top experts of the volcano, excluding themselves. Next, each expert selected the parameters that they believed were indicative of unrest, the magmatic origin of unrest, an impending eruption, and the location of the next vent opening, assigning each parameter a weight and the thresholds to define fuzzy anomalies (the parameters of Eqs. 1 and 2). The assignment of thresholds was optional because an expert may consider a parameter outside his or her expertise as indicative of a particular volcanic phenomenon, although he or she may not wish to express himself or herself a quantitative threshold: in this case, it was possible to rely on the choices made by the other experts.

The first step in post processing is to assign a weight (w_e) to each expert (Fig. 3). This weight is calculated as the sum of the votes each expert received. At this point the score (S) of each parameter is calculated, which is the sum of the weights of the experts who voted for it. After that, a consistency check is made by analyzing the results

obtained by considering the experts' weights (scores) or without considering them (votes). Score and vote series and statistics on thresholds and weights are checked analytically. This check shows consistency between the results obtained through the two procedures, however, the weighted procedure has smaller confidence intervals (10th-90th percentiles), as expected (Cooke, 1991).

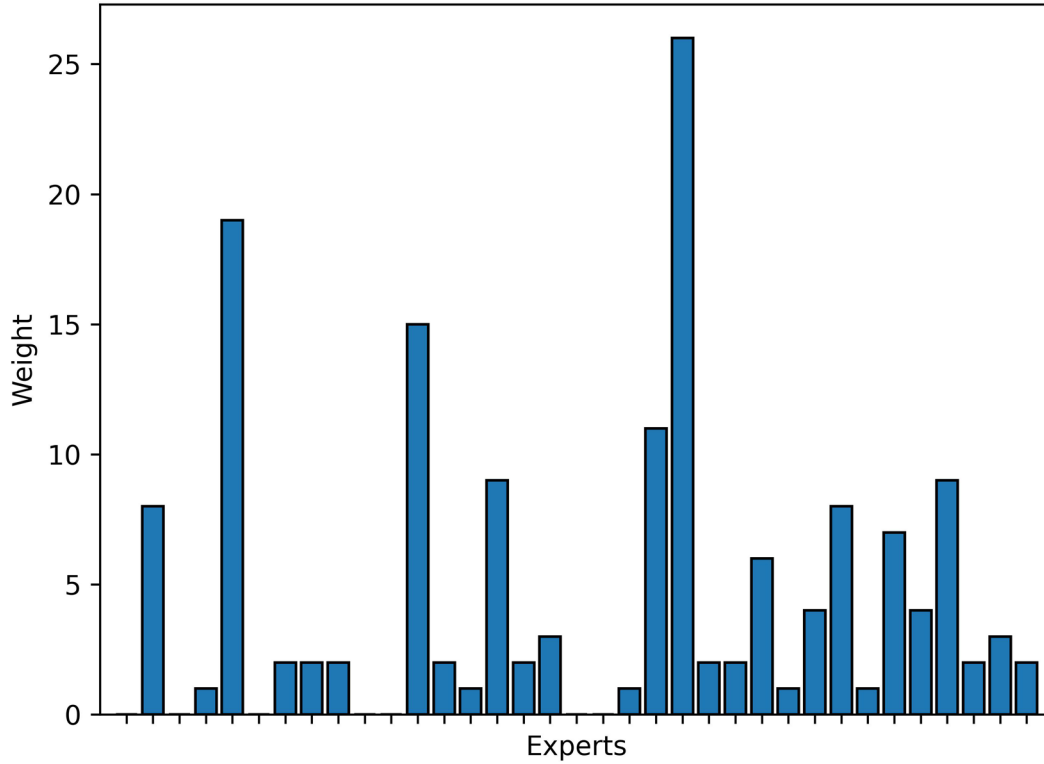


Figure 3. Weights of the experts (w_e) at Elicitation 6.

The most important parameters were defined by defining a minimum score. Acceptance thresholds are selected for each node at the maximum derivative of the score series, using a change-point search technique based on the Wilcoxon test (Selva and Marzocchi, 2005), with a significance level of $\alpha = 0.10$.

Elicitation 6 was held online the 16-23 February 2015, with the active participation of 35 experts (Selva et al., 2015). In Figs. 3 and 4, we report the experts' weights and the comparison between scores and votes for all the defined parameters, respectively. The selection of the parameters is based on their scores. No significant change-points were found at Node 1, this highlights how experts' opinions are discordant on the definition of operational unrest. Significant change-points were found instead at Nodes 2 and 3 at scores of 80, 55 and 23. The first two change-points ($S_m = 55$ and $S_M = 80$) were used to classify the parameters as high, intermediate and low score. The parameters with high score ($S > S_M$) were selected and the parameters with low score ($S < S_m$) were rejected. The weights of parameters having score $S_m < S < S_M$ are then multiplied by their respective probability of acceptance (Selva et al., 2012, 2015), which is given by:

$$p_a = \frac{S - S_m}{S_M - S_m} \quad (8)$$

Based on the found change points, the acceptance thresholds were set to 55 and 80. Next, the thresholds and the parameters weights of the accepted parameters (i.e., those with scores greater than 55) are selected as the weighted median (with experts' weights w_e , i.e., weighted through the experts' weights, so that the thresholds for each parameter are closer to those indicated by higher-weight experts) of the respective distributions. Tables 1, 2 and 3 present the results of the elicitation at the first three nodes of BET_EF, according to the rules explained.

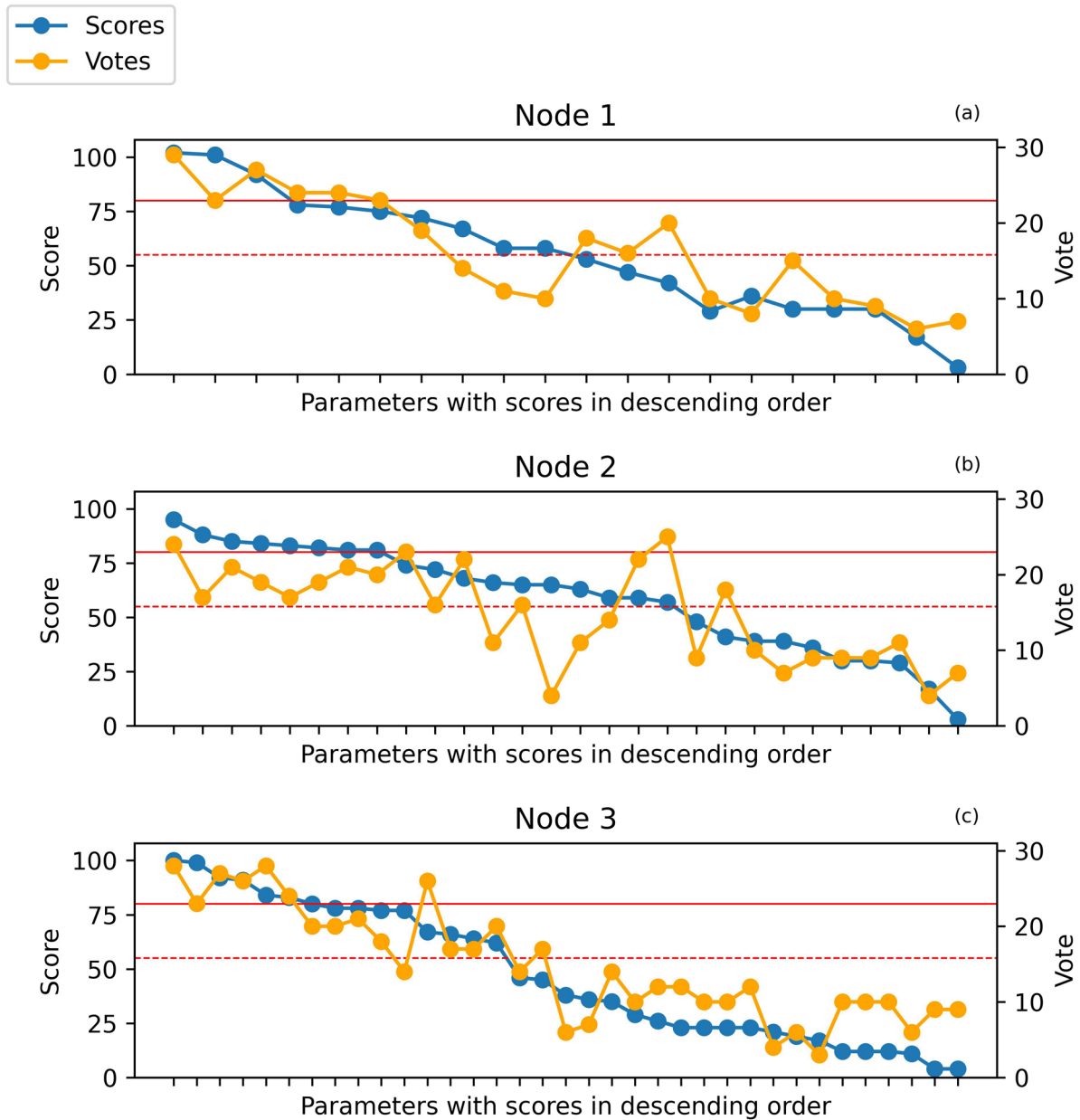


Figure 4. Series of scores and votes with parameters arranged in descending order according to the scores for (a) Node 1, (b) Node 2, (c) Node 3. The dashed red line represents the lower score threshold (S_m) while the solid red line represents the upper score threshold (S_M) (see Eq. 8).

These results highlight a consistent picture of what experts expect to see during unrest, right up to the time of the eruption. There is an increase in thresholds from Node 1 to Node 3, as expected, while parameters such as “phreatic activity” and “fractures” appear only at Node 3, as they are considered “major” parameters.

Parameter	Inertia	Unit	Thresholds	Weight
# VTs ($M > 0.8$)	(*)	ev/day	>5-20	—
# VTs ($z > 3.5$ km, $M > 0.8$)	(*)	ev/day	>1-3	—
Max magnitude	last month	—	>2.0-2.5	—

Parameter	Inertia	Unit	Thresholds	Weight
# LPs/ VLPs/ULPs	—	ev/month	>3-10	—
Tremor	last month	—	YES/NO	—
Uplift	cum. last 3 months	cm	>2-4.5	—
Uplift rate	last 3 months	cm/month	>0.85-1.4	—
Extension of outgassing structures or increase in flow	last month	—	YES/NO	—
Presence of acid gases (HF, HCl, SO ₂)	last 3 months	—	YES/NO	—

Table 1. List of parameters for evaluating the degree of unrest (Eq. 7) (INGV/DPC V2 project). By “inertia,” we mean the time during which an anomaly is considered active after its detection. The asterisk (*) represents the number of earthquakes divided by the number of days from the start of counting. This choice makes the inertia proportional to the number of earthquakes recorded (and to the total energy emitted); that is, the higher the number of earthquakes, the greater the inertia.

Parameter	Inertia	Unit	Thresholds	Weight
# VTs (M > 0.8)	(*)	ev/day	>10-50	1
# VTs (z > 3.5 km, M > 0.8)	(*)	ev/day	>2-10	1
Max magnitude	last month	—	>2.5-3	0.32
# LPs	(*)	ev/day	>2-20	1
# LPs (z > 2.0 km)	(*)	ev/day	>3-10	0.68
# VLPs/ULPs	(*)	ev/day	>1-5	0.92
# VLPs/ULPs (z > 2.0 km)	(*)	ev/month	>1-6	0.32
Tremor	last month	—	YES/NO	0.08
Tremor (z > 3.5 km)	last month	—	YES/NO	1
Uplift	cum. last 3 months	cm	>10-30	1
Uplift rate	last 3 months	cm/month	>3-10	0.88
Significant variations in the V _{up} at RITE and V _{up} at other stations ratio ⁽¹⁾⁽²⁾	last month	—	YES/NO	0.4
Significant variations in the V _{hor} /V _{up} ratio at any station ⁽¹⁾⁽²⁾	last month	—	YES/NO	1
Peak of uplift rate at station other than RITE ⁽¹⁾	last month	—	YES/NO	0.16
Extension of outgassing structures or increase in flow	last month	—	YES/NO	0.16

(¹) Only for V_{up} > 3 cm/month. (²) By “significant,” we mean outside of the noise.

Parameter	Inertia	Unit	Thresholds	Weight
Presence of acid gases (HF, HCl, SO ₂)	last 3 months	—	YES/NO	0.76
Variation of the magmatic component	last month	—	YES/NO	0.52
Variation of gases composition	last month	—	YES/NO	0.4

(¹) Only for Vup > 3 cm/month. (²) By “significant,” we mean outside of the noise.

Table 2. List of parameters for assessing the probability of magmatic unrest (INGV/DPC V2 project). The asterisk (*) represents the number of earthquakes divided by the number of days from the start of counting.

Parameter	Inertia	Unit	Thresholds	Weight
RSAM acceleration	last week	—	YES/NO	1
Acceleration in the # of seismic events	last week	—	YES/NO	0.48
Acceleration in seismic energy released	last week	—	YES/NO	1
Tremor	last month	—	YES/NO	1
Tremor (z > 2.0 km)	last month	—	YES/NO	0.28
Uplift	last 3 months	cm	>20-100	0.44
Uplift rate	last 3 months	cm/day	>5-10	0.44
Significant variations in the Vup at RITE and Vup at other stations ratio (¹)(²)	last month	—	YES/NO	0.44
Significant variations in the Vhor/Vup ratio at any station (¹)(²)	last month	—	YES/NO	1
Peak of uplift rate at station other than RITE (¹)	last month	—	YES/NO	0.92
New significant fractures	last 3 months	—	YES/NO	1
Presence of acid gases (HF, HCl, SO ₂)	last week	—	YES/NO	1
New hydrothermal springs	last week	—	YES/NO	0.92
Phreatic activity	last week	—	YES/NO	1
Sudden stop in seismicity and/or deformation	last week	—	YES/NO	0.36

(¹) Only for Vup > 3 cm/month. (²) By “significant,” we mean outside of the noise.

Table 3. List of parameters for assessing the probability of eruption within one month (INGV/DPC V2 project). The symbolism is the same as that used in Tables 1 and 2.

Using the same thresholds adopted for the first three nodes, none of the parameters at Node 4 is selected. This is due to the fact that many experts did not fill out the form related to that specific node, and many selections were divided among slightly different parameters. The most important parameters were deformation, phreatic activity, new fumaroles and VT seismicity combined with depth (Table 4), which were selected by merging such different parameters.

Parameter	Inertia	Rank
Peak of uplift rate at station other than RITE ⁽¹⁾	last month	1
Phreatic activity	last week	2
New hydrothermal springs	last week	3
New significant fractures	last 3 months	4
Significative variations in the V_{hor}/V_{up} ratio at any station ⁽¹⁾⁽²⁾	last month	5
Hypocenter dispersion (vertical: distance between 10 and 90 percentile)	last week	6
Restricted seismogenic volumes	last week	7
Tremor	last month	8
Uplift	cum. last 3 months	9
Significative variations in the V_{hor}/V_{up} ratio at any station ⁽¹⁾⁽²⁾	last month	10
# LPs ($z < 2.0$ km)	(*)	11
# VTs ($z < 3.5$ km, $M > 0.8$)	(*)	12
RSAM acceleration	last week	13
# VLPs/ULPs ($z > 2.0$ km)	(*)	14
Seismic events in areas previously of low seismicity	last month	15
⁽¹⁾ Only for $V_{up} > 3$ cm/month. ⁽²⁾ By “significant,” we mean outside of the noise.		

Table 4. List of parameters for assessing the probability of vent opening (INGV/DPC V2 project). The symbolism is the same as that used in Tables 1, 2 and 3.

4. Tracking the evolution of the current unrest of Campi Flegrei

Since the beginning of the ongoing uplift phase of Campi Flegrei, that started in 2005, the strongest signs of unrest have been observed between the beginning of 2023 and the time of writing this article (June 2024). The alert level was raised to ‘yellow’ in 2012, when the activity started being more significant with uplift, increased seismicity, changes in the geochemical composition of fumaroles and gases coming from the ground (<https://rischi.protezionecivile.gov.it/it/vulcanico/vulcani-italia/campi-flegrei/>). From January 2023 the monitoring system of INGV (Istituto Nazionale di Geofisica e Vulcanologia) has recorded a total of more than 9000 seismic events and a cumulative uplift of more than 25 cm in the area of maximum deformation, while the geochemical parameters indicate the continuation of trends previously identified.

We downloaded seismicity data from the GOSSIP database (<https://terremoti.ov.ingv.it/gossip/>), while for geodesy we used the weekly solutions from the GNSS stations located in the caldera area (De Martino et al., 2021), assuming the linearity of deformation between solutions.

The concern of the population was mostly raised by the 2023–2024 seismic activity. Indeed, many seismic swarms occurred during this period, and despite the relatively low-to-moderate magnitude of the events ($maxM_d = 4.4$ on 20 May 2024), the population felt a good proportion of them due to their shallow hypocentral depth. The most intense seismic activity was concentrated in the months between August and October 2023 and in April and May 2024. During 2023, among the numerous seismic swarms, three particularly increased the level of concern among the citizens of the Campi Flegrei area. The first swarm started on 17 August 2023, characterized by 115 events

with $M_d \geq 0.0$ and a maximum magnitude of $M_d = 3.6$. The second one began on 26 September 2023, with 88 events of magnitude $M_d \geq 0.0$ and a maximum magnitude of $M_d = 4.2$. The third one started on 2 October 2023, involving 35 events with $M_d \geq 0.0$ and a maximum magnitude of $M_d = 4.0$. Seismicity further intensified between the months of April and May 2024. Specifically, 14 earthquake swarms occurred in April 2024, with the highest magnitude event ($M_d = 3.9$) occurring on 27 April 2024. Among the 11 seismic swarms that occurred in May 2024, there was one that especially caused concern among the people in the area. This swarm began on the evening of 20 May 2024, it was characterized by 252 events of magnitude $M_d \geq 0.0$ and a maximum magnitude of $M_d = 4.4$, which corresponds to the highest magnitude ever recorded at Campi Flegrei in instrumental time.

Within this time frame, the degree of unrest, calculated according to Eq. (7), has always been equal to 1, due to the value of the parameter “Uplift Rate” that has always been higher than the upper threshold that defines its anomalous values at Node 1 (Table 1).

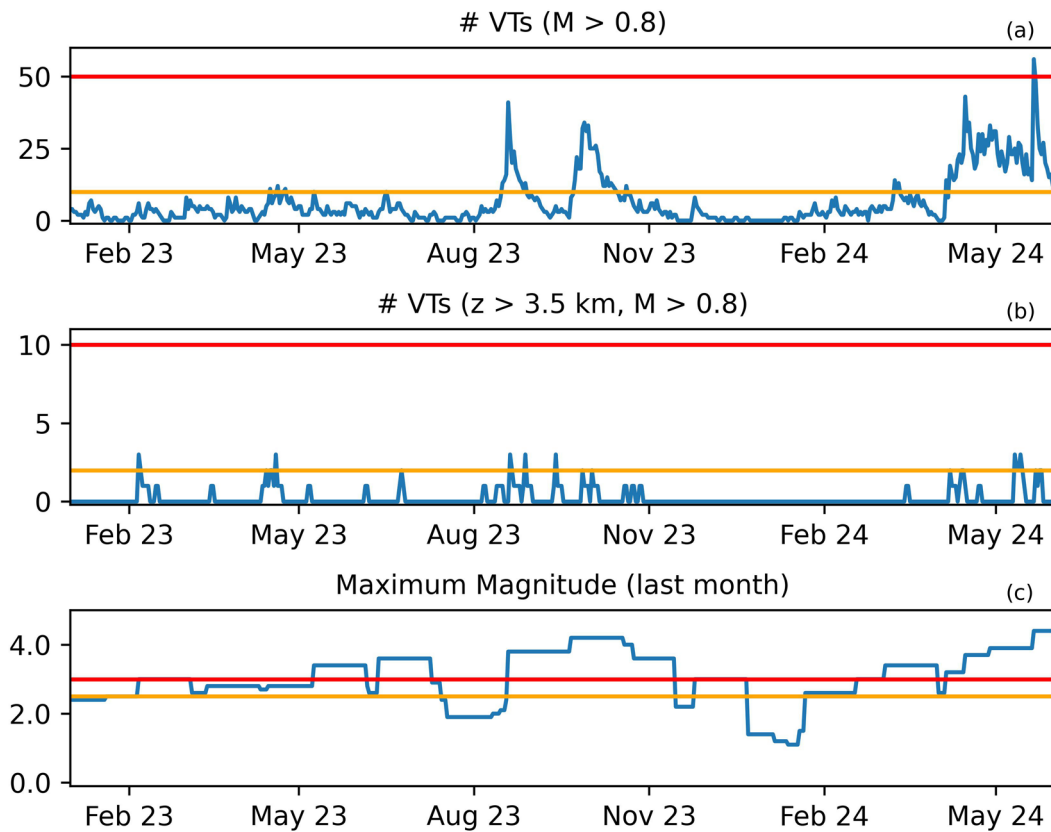


Figure 5. Variation of parameters related to Node 2 of the BET (magmatic unrest) that exhibited an anomaly degree greater than 0 during the studied period. (a) Daily number of VTs. (b) Daily number of deep VTs. (c) Maximum magnitude (last month). The orange and red lines represent the lower and upper thresholds that define the anomalous values of the parameters, respectively (see Table 2).

Figure 5 shows the variation of all parameters indicative of shallow magma intrusion (Table 2) that have exhibited a degree of anomaly ($z > 0$) at least once (see Eq. 1). The plot highlights that the parameter related to the number of VTs has repeatedly exceeded the lower anomaly threshold, and it has also exceeded the upper threshold after the 20 May 2024 seismic swarm. Also, the parameter related to the number of deep VTs has exceeded the lower threshold on different occasions. Conversely, the “Maximum Magnitude” parameter has been at least partially anomalous for most of the application, and it has also exceeded the upper threshold on many different occasions. The parameters related to long-period seismicity have never exceeded the corresponding lower thresholds, while seismic tremor, on the other hand, has not been detected. Regarding parameters related to geodesy and geochemistry, no anomalies linked to a potential shallow magma movement have been detected.

No anomalies associated with the pre-eruptive phase (Table 3) have been detected throughout the entire examined period.

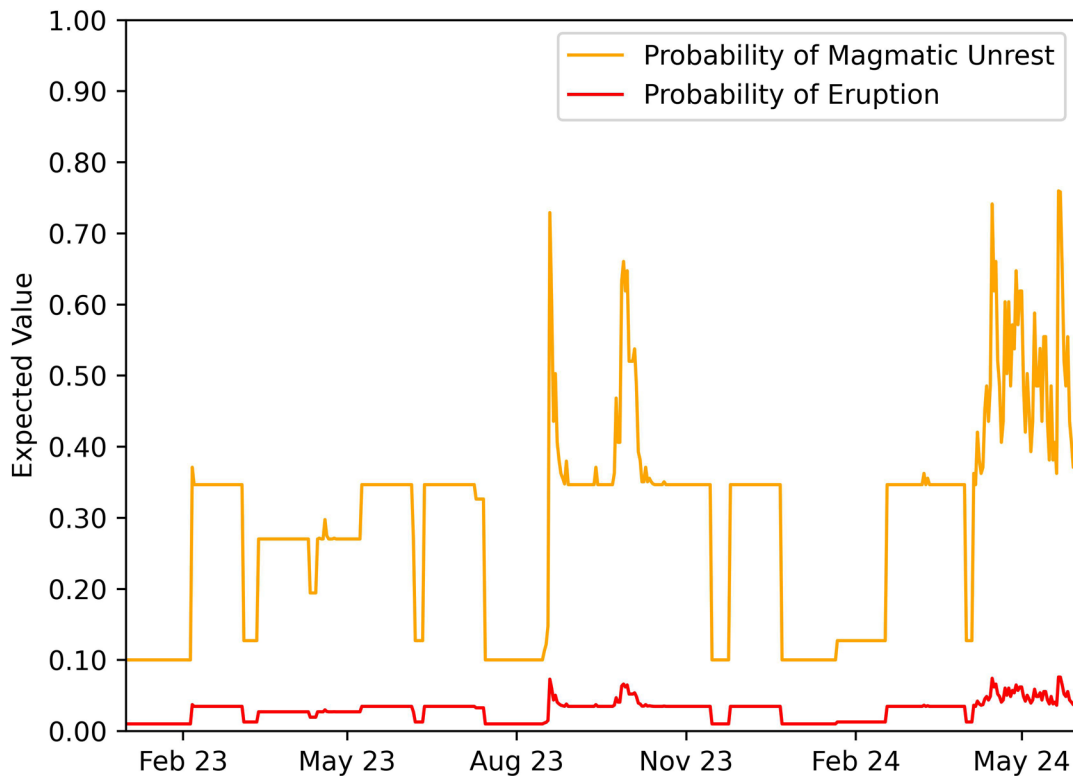


Figure 6. Variation of the expected value of the probability of Magmatic Unrest (orange line) and Eruption within a one-month time window (red line) throughout the entire examined period.

Figure 6 illustrates the variation of the best guess (the mean of the beta distribution) probability of magmatic unrest and eruption within a one-month time window, throughout the entire application. The figure highlights that the probability of magmatic unrest was lower than that of unrest of another nature for most of the time. The probability of magmatic unrest surpassed the probability of unrest of another nature on different occasions. The figure highlights that the probability of magmatic unrest was lower than that of unrest of another nature for most of the application, except during a few occasions. The first one was on 18 August 2023, while the second one was on 27 September 2023. The probability of magmatic unrest returned to the background level in December due to the inertia of the “Maximum Magnitude” parameter (Table 2), one month after the last earthquake with anomalous magnitude of the year 2023, that occurred on 23 November 2023.

The probability of magmatic unrest remained at the background value until 21 January 2024, when a magnitude $M_d = 2.6$ earthquake occurred. After that, the probability of magmatic unrest never returned to the background level. The probability of magmatic unrest exceeded again the probability of unrest of another nature on different occasions starting from the month of April 2024, due to the increase of seismicity that we mentioned before (Fig. 5).

The variations of the probability of eruption are simply a consequence of the variations in the probability of magmatic unrest, as no anomalies were observed at Node 3 of BET_EF. The probability of eruption corresponds to one-tenth of the probability of magmatic unrest since we used a value of $a = 0.9$ (see Eq. 3).

As previously explained in Section 2, the trends shown in Fig. 6 represent the variation of the expected value of a beta distribution. The related uncertainty is set by setting the parameter λ (see Eq. 6). Following Marzocchi et al. (2024) we set $\lambda = 10$, and the obtained uncertainty is reported with the distribution of 10th, 50th, and 90th percentiles in Fig. 7. Such percentiles are evaluated from the beta distribution, which is displayed entirely in Fig. 8 for the 20 May 2024, when the absolute probability of magmatic unrest and eruption was maximum. On that day the probability of magmatic unrest ranged from 0.59 (10th percentile) to 0.91 (90th percentile), while the monthly probability of eruption ranged from 0.01 (10th percentile) to 0.17 (90th percentile).

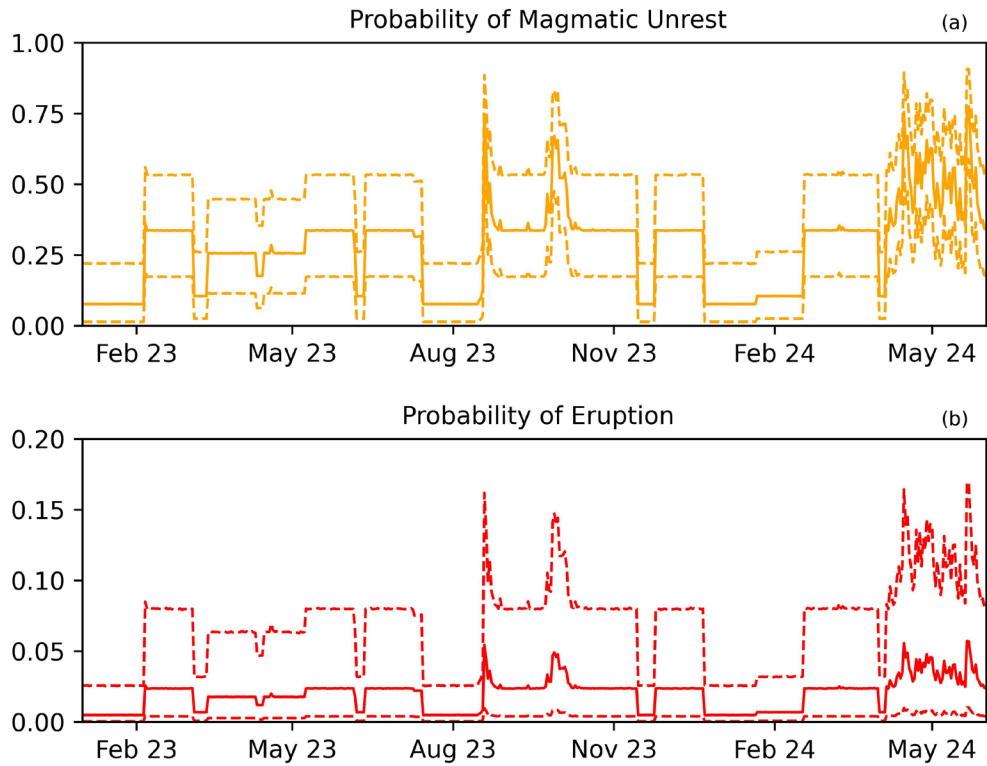


Figure 7. Variation of the median (solid lines) and 10th and 90th percentiles (dashed lines) of the probability distributions of Magmatic Unrest (a) and Eruption within a one-month time window (b).

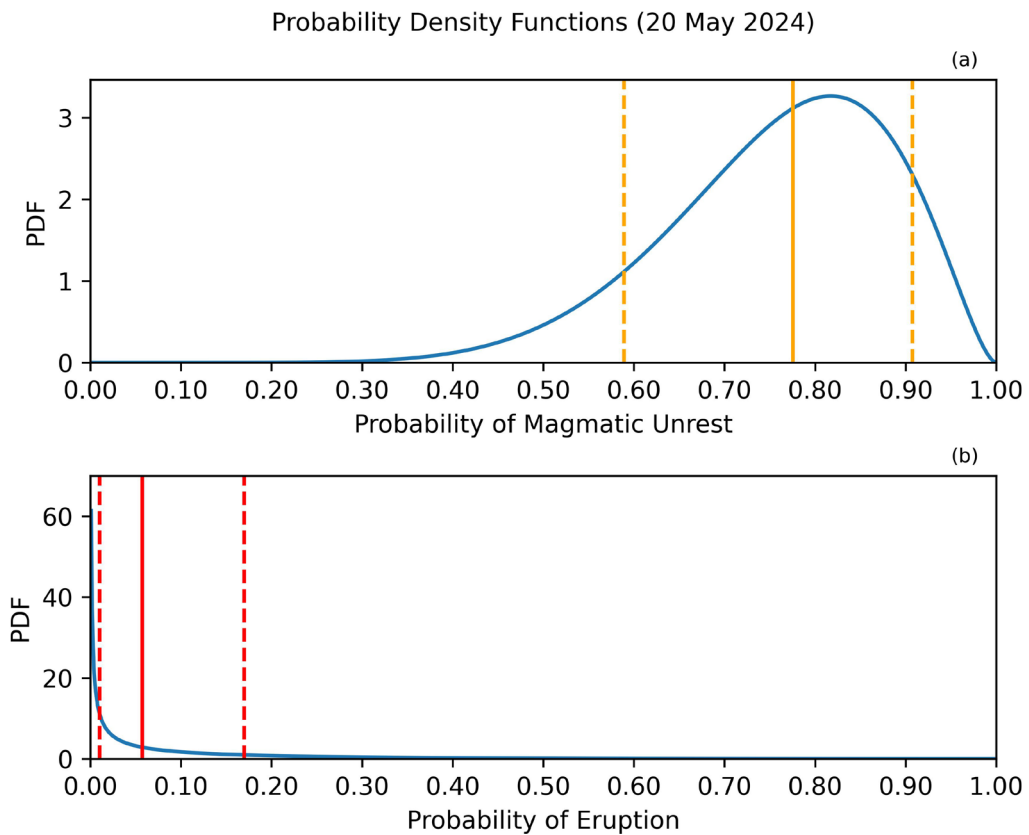


Figure 8. Probability Density Functions of Magmatic Unrest (a) and Eruption within a one-month time window (b) related to 20 May 2024 ($E[\Phi_2] = 0.76$, $E[\Phi_3] = 0.076$). The vertical solid lines depict the medians of the distributions, while the dashed lines represent the 10th and 90th percentiles.

5. Conclusions and perspectives

Volcanologists often rely on a highly subjective interpretation of precursor phenomena, typically expressed in terms of alert levels. However, we argue that the use of an alert level-based system is often uninformative, partly because a specific alert level does not precisely quantify the hazard, and partly because it relies on pre-determined patterns of precursor phenomena (Marzocchi et al., 2006, 2021; Papale, 2017).

The use of BET_EF allows for an explicit management of the uncertainty. The use of probabilities allows also for the definition of quantitative protocols that facilitate decision-making processes (Marzocchi and Woo, 2007). Additionally, defining parameters and their respective thresholds in advance of a crisis through the elicitation process (Selva et al., 2012) enables a more flexible and authoritative analysis of precursors, as the BET_EF structure allows considering, at each node, all possible combinations of phenomena that may suggest the magmatic origin of unrest and eruption.

Here, we have seen the interpretation of the ongoing unrest episode at Campi Flegrei using the shared picture of its behavior evaluated through an experts' elicitation that was held before the beginning of the present-day crisis. To our knowledge, this is the only forecasting tool that has been available since the beginning of the unrest. This picture summarizes the opinion of the entire group of 35 experts of Campi Flegrei.

The results show that:

- Models like BET_EF, calibrated through the elicitation process, are currently the only way to track the evolution of volcanic unrest quantitatively and automatically in real-time based on the opinion of a large community of experts.
- The probability of magmatic unrest was lower than that of unrest of other origins for most of the time. This trend reversed in August and at the end of September 2023, and in April and May 2024.
- At the end of the examined period the probability of magmatic unrest is still higher than the background level.
- There is no evidence of anomalies characteristic of a pre-eruptive phase.

Finally, we would like to point out that experts' elicitation is a continuous process, as long as our knowledge about the system and data are continuously increasing. Owing to the long time elapsed since the VI elicitation we are currently working on the outcomes of the VII elicitation for Campi Flegrei. Hence, this example has the main purpose to show how the BET can assist decision makers to achieve defensible risk reduction solutions. Its huge societal value consists on the fact that the BET outcomes do not represent the view of its authors or of one single researcher, but they reflect the perspective of the scientific community that took part in the elicitation process over the years, involving more than 100 researchers across all elicitation phases until the VI one that took place in 2015.

Data availability statement. Information regarding the evolution of Campi Flegrei unrest was extracted from the weekly and monthly bulletins of the Campi Flegrei provided by the Istituto Nazionale Geofisica e Vulcanologia (INGV) – Osservatorio Vesuviano: <https://www.ov.ingv.it/index.php/monitoraggio-e-infrastrutture/bollettini-tutti>.

The seismicity data were extracted from the GOSSIP database, also provided by the Istituto Nazionale Geofisica e Vulcanologia (INGV) – Osservatorio Vesuviano: <https://terremoti.ov.ingv.it/gossip/flegrei/>.

Information regarding alert levels for Campi Flegrei can be found on the Dipartimento della Protezione Civile (DPC) website at the following link: <https://rischi.protezionecivile.gov.it/it/vulcanico/vulcani-italia/campi-flegrei/>.

Appendix. In addition to the authors, the members of the Elicitation VI Working Group contributed to the creation of this paper by taking an active part in the VI Elicitation of Campi Flegrei:

Valerio Acocella, Matteo Bagagli, Francesca Bianco, Sven Borgstrom, Stefano Caliro, Bruno Capaccioni, Mario Castellano, Giovanni Chiodini, Luca Crescentini, Luca D'Auria, Massimo D'Antonio, Walter De Cesare, Prospero De Martino, Edoardo Del Pezzo, Antonietta Esposito, Danilo Galluzzo, Deepak Garg, Flora Giudicepietro, Mario La Rocca, Antonella Longo, Annarita Mangiacapra, Warner Marzocchi, Chiara Montagna, Massimo Orazi, Paolo Papale, Rosario Peluso, Zaccaria Petrillo, Simona Petrosino, Patrizia Ricciolino, Dmitri Rouwet, Laura Sandri, Roberto Scarpa, Umberto Tammaro, Micol Todesco, Lucia Zaccarelli.

Acknowledgements. This work benefited from the agreement between Istituto Nazionale di Geofisica e Vulcanologia (INGV) and the Italian Presidenza del Consiglio dei Ministri, Dipartimento della Protezione Civile (DPC). We thank Paolo

Papale who, as Director of the Volcano Section of INGV, formed the Working Group that authored this research. This paper does not necessarily represent DPC official opinion and policies.

The authors wish to thank the Editor Annalisa Cappello and two anonymous reviewers who have spent time and knowledge to provide comments and suggestions that have improved the quality of the manuscript.

References

- Acocella, V., M. Ripepe, E. Rivalta, A. Peltier et al. (2024). Towards scientific forecasting of magmatic eruptions, *Nat. Rev. Earth Environ.*, 5, 1, 5-22, doi:10.1038/s43017-023-00492-z.
- Aspinall, W. P. (2006). Structured elicitation of expert judgement for probabilistic hazard and risk assessment in volcanic eruptions, *Statistics in Volcanology*, 1, 15-30, doi:10.1144/IAVCEI001.2.
- Bevilacqua, A., F. Flandoli, A. Neri, R. Isaia et al. (2016). Temporal models for the episodic volcanism of Campi Flegrei caldera (Italy) with uncertainty quantification, *J. Geophys. Res. Solid Earth*, 121, 11, 7821-7845, doi:10.1002/2016JB013171.
- Bevilacqua, A., A. Neri, P. De Martino, F. Giudicepietro et al. (2024). Accelerating upper crustal deformation and seismicity of Campi Flegrei caldera (Italy), during the 2000-2023 unrest, *Commun. Earth Environ.*, 5, 1, 1-14, doi:10.1038/s43247-024-01865-y.
- Chiodini, G., A. Paonita, A. Aiuppa, A. Costa et al. (2016). Magmas near the critical degassing pressure drive volcanic unrest towards a critical state, *Nat. Commun.*, 7, 1, 13712, doi:10.1038/ncomms13712.
- Chiodini, G., J. Selva, E. Del Pezzo, D. Marsan et al. (2017). Clues on the origin of post-2000 earthquakes at Campi Flegrei caldera (Italy), *Sci. Rep.*, 7, 1, 4472, doi:10.1038/s41598-017-04845-9.
- Chiodini, G., S. Caliro, R. Avino, G. Bini et al. (2021). Hydrothermal pressure-temperature control on CO₂ emissions and seismicity at Campi Flegrei (Italy), *J. Volcanol. Geotherm. Res.*, 414, 107245, doi:10.1016/j.jvolgeoes.2021.107245.
- Christophersen, A., N. I. Deligne, A. M. Hanea, L. Chardot et al. (2018). Bayesian network modeling and expert elicitation for probabilistic eruption forecasting: Pilot study for Whakaari/White Island, New Zealand, *Front. Earth Sci.*, 6, 211, doi:10.3389/feart.2018.00211.
- Cooke, R. (1991). *Experts in uncertainty: opinion and subjective probability in science*, Oxford University Press, USA, doi:10.1086/293541.
- D'Auria, L., F. Giudicepietro, I. Aquino, G. Borriello et al. (2011). Repeated fluid-transfer episodes as a mechanism for the recent dynamics of Campi Flegrei caldera (1989-2010), *J. Geophys. Res. Solid Earth*, 116, B4, doi:10.1029/2010JB007837.
- D'Auria, L., S. Pepe, R. Castaldo, F. Giudicepietro et al. (2015). Magma injection beneath the urban area of Naples: a new mechanism for the 2012-2013 volcanic unrest at Campi Flegrei caldera, *Sci. Rep.*, 5, 1, 13100, doi:10.1038/srep13100.
- De Martino, P., M. Dolce, G. Brandi, G. Scarpato et al. (2021). The ground deformation history of the Neapolitan volcanic area (Campi Flegrei caldera, Somma-Vesuvius volcano, and Ischia island) from 20 years of continuous GPS observations (2000-2019), *Remote Sens.*, 13, 14, 2725, doi:10.3390/rs13142725.
- Di Vito, M., L. Lirer, G. Mastrolorenzo and G. Rolandi (1987). The 1538 Monte Nuovo eruption (Campi Flegrei, Italy), *Bull. Volcanol.*, 49, 608-615, doi:10.1007/BF01079966.
- Di Vito, M. A., V. Acocella, G. Aiello, D. Barra et al. (2016). Magma transfer at Campi Flegrei caldera (Italy) before the 1538 AD eruption, *Sci. Rep.*, 6, 1, 32245, doi:10.1038/srep32245.
- Fernandez, G., B. Giaccio, A. Costa, L. Monaco et al. (2024). New constraints on the Middle-Late Pleistocene Campi Flegrei explosive activity and Mediterranean tephrostratigraphy (~160 ka and 110-90 ka), *Quat. Sci. Rev.*, 331, 108623, doi:10.1016/j.quascirev.2024.108623.
- Gelman, A., J. B. Carlin, H. S. Stern and D. B. Rubin (1995). *Bayesian data analysis*, Chapman and Hall/CRC, doi:10.1201/9780429258411.
- Giudicepietro, F., G. Chiodini, R. Avino, G. Brandi et al. (2020). Tracking episodes of seismicity and gas transport in Campi Flegrei caldera through seismic, geophysical, and geochemical measurements, *Seismol. Res. Lett.*, 92, 2A, 965-975, doi:10.1785/0220200223.
- Giudicepietro, F., P. Ricciolino, F. Bianco, S. Caliro et al. (2021). Campi Flegrei, Vesuvius and Ischia seismicity in the context of the Neapolitan volcanic area, *Front. Earth Sci.*, 9, 662113, doi:10.3389/feart.2021.662113.

- Guidoboni, E. and C. Ciuccarelli (2011). The Campi Flegrei caldera: historical revision and new data on seismic crises, bradyseisms, the Monte Nuovo eruption and ensuing earthquakes (twelfth century 1582 AD), *Bull. Volcanol.*, 73, 655-677, doi:10.1007/s00445-010-0430-3.
- Isaia, R., M. G. Di Giuseppe, J. Natale, F. D. A. Tramparulo et al. (2021). Volcano-tectonic setting of the Pisciarelli fumarole field, Campi Flegrei caldera, southern Italy: Insights into fluid circulation patterns and hazard scenarios, *Tectonics*, 40, 5, doi:10.1029/2020TC006227.
- Lima, A., R. J. Bodnar, B. De Vivo, F. J. Spera et al. (2021). Interpretation of recent unrest events (Bradyseism) at Campi Flegrei, Napoli (Italy): comparison of models based on cyclical hydrothermal events versus shallow magmatic intrusive events, *Geofluids*, 2021, 1-16, doi:10.1155/2021/2000255.
- Marzocchi, W., L. Sandri, P. Gasparini, C. Newhall et al. (2004). Quantifying probabilities of volcanic events: the example of volcanic hazard at Mount Vesuvius, *J. Geophys. Res. Solid Earth*, 109, B11, doi:10.1029/2004JB003155.
- Marzocchi, W., L. Sandri and C. Furlan (2006). A quantitative model for volcanic hazard assessment, in *Statistics in Volcanology*, H. M. Mader, S. G. Coles, C. B. Connor and L. J. Connor, Geological Society of London, doi:10.1144/IAVCEI001.3.
- Marzocchi, W. and G. Woo (2007). Probabilistic eruption forecasting and the call for an evacuation, *Geophys. Res. Lett.*, 34, 22, doi:10.1029/2007GL031922.
- Marzocchi, W., L. Sandri and J. Selva (2008). BET_EF: a probabilistic tool for long- and short-term eruption forecasting, *Bull. Volcanol.*, 70, 623-632, doi:10.1007/s00445-007-0157-y.
- Marzocchi, W. and G. Woo (2009). Principles of volcanic risk metrics: Theory and the case study of Mount Vesuvius and Campi Flegrei, Italy, *J. Geophys. Res. Solid Earth*, 114, B3, doi:10.1029/2008JB005908.
- Marzocchi, W. and M. S. Bebbington (2012). Probabilistic eruption forecasting at short and long time scales, *Bull. Volcanol.*, 74, 1777-1805, doi:10.1007/s00445-012-0633-x.
- Marzocchi, W., J. Selva and T. H. Jordan (2021). A unified probabilistic framework for volcanic hazard and eruption forecasting, *Nat. Hazards Earth Syst. Sci.*, 21, 11, 3509-3517, doi:10.5194/nhess-21-3509-2021.
- Marzocchi, W., P. Papale, L. Sandri and J. Selva (2021). Reducing the volcanic risk in the frame of the hazard/risk separation principle, in *Forecasting and Planning for Volcanic Hazards, Risks, and Disasters* G. Valentine (Ed.), Elsevier, 545-564, doi:10.1016/B978-0-12-818082-2.00014-7.
- Marzocchi, W., L. Sandri, S. Ferrara and J. Selva (2024). From the detection of monitoring anomalies to the probabilistic forecast of the evolution of volcanic unrest: an entropy-based approach, *Bull. Volcanol.*, 86, 1, 5, doi:10.1007/s00445-023-01692-7.
- Orsi, G., L. Civetta, C. Del Gaudio, S. De Vita et al. (1999). Short-term ground deformations and seismicity in the resurgent Campi Flegrei caldera (Italy): an example of active block-resurgence in a densely populated area, *J. Volcanol. Geotherm. Res.*, 91, 2-4, 415-451, doi:10.1016/S0377-0273(99)00050-5.
- Orsi, G., M. A. Di Vito, J. Selva and W. Marzocchi (2009). Long-term forecast of eruption style and size at Campi Flegrei caldera (Italy), *Earth Planet. Sci. Lett.*, 287, 1-2, 265-276, doi:10.1016/j.epsl.2009.08.013.
- Parascandola, A. (1947). I fenomeni bradisismici del Serapeo di Pozzuoli, Stabilimento tipografico G. Genovese.
- Papale, P. (2017). Rational volcanic hazard forecasts and the use of volcanic alert levels, *J. Appl. Volcanol.*, 6, 1, 13, doi:10.1186/s13617-017-0064-7.
- Ricciolino, P. and D. Lo Bascio (2021). Cataloghi sismici dei vulcani campani. Stazione STH Campi Flegrei dal 2000 al 2021 (Cat-STH_2000_2021), Istituto Nazionale di Geofisica e Vulcanologia, Data set, doi:10.13127/ovcatalogsth_2000_2021.
- Ricco, C., S. Petrosino, I. Aquino, C. Del Gaudio et al. (2019). Some investigations on a possible relationship between ground deformation and seismic activity at Campi Flegrei and Ischia volcanic areas (Southern Italy), *Geosci.*, 9, 5, 222, doi:10.3390/geosciences9050222.
- Rosi, M., V. Acocella, R. Cioni, F. Bianco et al. (2022). Defining the pre-eruptive states of active volcanoes for improving eruption forecasting, *Front. Earth Sci.*, 10, doi:10.3389/feart.2022.795700.
- Scarpati, C., A. Perrotta, S. Lepore and A. Calvert (2013). Eruptive history of Neapolitan volcanoes: constraints from ⁴⁰Ar-³⁹Ar dating, *Geol. Mag.*, 150, 3, 412-425, doi:10.1017/S0016756812000854.
- Selva, J. and W. Marzocchi (2005). Variations of southern California seismicity: Empirical evidence and possible physical causes, *J. Geophys. Res. Solid Earth*, 110, B11, doi:10.1029/2004JB003494.
- Selva, J., W. Marzocchi, P. Papale and L. Sandri (2012). Operational eruption forecasting at high-risk volcanoes: the case of Campi Flegrei, Naples, *J. Appl. Volcanol.*, 1, 1-14, doi:10.1186/2191-5040-1-5.

- Selva, J., L. Sandri, M. Cincini and P. Perfetti (2015). Aggiornamento dell'albero degli eventi. Elicitazione su parametri, soglie e loro combinazioni, Deliverable 2.1 del Progetto INGV/DPC V2 2012-2015.
- Smith, V. C., R. Isaia and N. J. G. Pearce (2011). Tephrostratigraphy and glass compositions of post-15 kyr Campi Flegrei eruptions: implications for eruption history and chronostratigraphic markers, *Quat. Sci. Rev.*, 30, 25-26, 3638-3660, doi:10.1016/j.quascirev.2011.07.012.
- Sparice, D., C. Pelullo, S. de Vita, I. Arienzo et al. (2024). The pre-Campi Flegrei caldera (>40 ka) explosive volcanic record in the Neapolitan Volcanic Area: New insights from a scientific drilling north of Naples, southern Italy, *J. Volcanol. Geotherm. Res.*, 455, doi:10.1016/j.jvolgeores.2024.108209.
- Todesco, M., A. Costa, A. Comastri, F. Colleoni et al. (2014). Vertical ground displacement at Campi Flegrei (Italy) in the fifth century: Rapid subsidence driven by pore pressure drop, *Geophys. Res. Lett.*, 41, 5, 1471-1478, doi:10.1002/2013GL059083.
- Tramelli, A., C. Godano, P. Ricciolino, F. Giudicepietro et al. (2021). Statistics of seismicity to investigate the Campi Flegrei caldera unrest, *Sci. Rep.*, 11, 1, 7211, doi:10.1038/s41598-021-86506-6.
- Tramelli, A., F. Giudicepietro, P. Ricciolino and G. Chiodini (2022). The seismicity of Campi Flegrei in the context of an evolving long term unrest, *Sci. Rep.*, 12, 1, 2900, doi:10.1038/s41598-022-06928-8.
- Tramelli, A., V. Convertito and C. Godano (2024). b value enlightens different rheological behaviour in Campi Flegrei caldera, *Commun. Earth Environ.*, 5, 1, 275, doi:10.1038/s43247-024-01447-y.
- Trasatti, E., M. Polcari, M. Bonafede and S. Stramondo (2015). Geodetic constraints to the source mechanism of the 2011-2013 unrest at Campi Flegrei (Italy) caldera, *Geophys. Res. Lett.*, 42, 10, 3847-3854, doi:10.1002/2015GL063621.
- Vineberg, S. O., R. Isaia, P. G. Albert, R. J. Brown et al. (2023). Insights into the explosive eruption history of the Campanian volcanoes prior to the Campanian Ignimbrite eruption, *J. Volcanol. Geotherm. Res.*, 443, 107915, doi:10.1016/j.jvolgeores.2023.107915.
- Vitale, S. and J. Natale (2023). Combined volcano-tectonic processes for the drowning of the Roman western coastal settlements at Campi Flegrei (southern Italy), *Earth Planets Space*, 75, 1, 38, doi:10.1186/s40623-023-01795-7.
- Zadeh, L. A. (1965). Fuzzy sets, *Inf. Control.*, 8, 3, 338-353, doi:10.1016/S0019-9958(65)90241-X.

***CORRESPONDING AUTHOR: Jacopo SELVA,**

Università Federico II di Napoli, Dipartimento di Scienze della Terra, dell'Ambiente e delle Risorse,
Via Vicinale Cupa Cintia, 80126 Napoli, Italy
e-mail: jacopo.selva@unina.it